ARMA 13-100

A New Modeling Approach to Natural Fracturing Process

Chukwudozie, C., Bourdin, B.,
Louisiana State University, Baton Rouge, LA, USA
Yoshioka, K., Buchmann, T. and Connolly, P.
Chevron Energy Technology, Houston, TX, USA

This paper was prepared for presentation at the 47th US Rock Mechanics / Geomechanics Symposium held in San Francisco, CA, USA, 23-26 June 2013.

ABSTRACT: Robust understanding of natural fracture distribution and connectivity is crucial in hydrocarbon and geothermal energy development. Unfortunately, such characterization of the fractured formation remains a major challenge to the industry.
We propose the variational approach to fracture modelling, which provides a unified framework for studying fracture nucleation and initiation, autonomous propagation and the growth of an arbitrary number of fractures. In this study, we model fracture nucleation and the sequential infill fracturing of an entire brittle layer, as reported by several authors of out-crop based studies. In addition, the relationship between mechanical stratigraphy and fracture density is captured by studying the effect of the mechanical properties of the fracturing and non fracturing layers on the distribution of fractures within the brittle layers. From a parametric analysis, it is found that the mechanical properties and geometry have a strong effect on the density, spacing and overall distribution of fractures and the initiation of bedding parallel slip.

1. INTRODUCTION

Although fractured reservoirs hold a large percentage of the world's oil reserves, characterization and quantitative modeling of natural fractures remains a major challenge for the industry. This challenge is result of the complexities of fractures, the uniqueness in which they respond in different reservoirs and over-simplistic approaches in the description of fracture shapes and distributions (Nelson 2001). Despite these challenges, it is important to incorporate the effect of natural fractures at the outset of field developments as ignoring their influence may have significant consequences.

Understanding the characteristics of natural fractures is a first step towards robustly incorporating fractures into a field development design. It is generally understood that natural fractures are dependent on the mechanical stratigraphy of sedimentary rocks. In fact, Becker *et al*. (1996) reported that in fairly undeformed rocks, fracture height and intensity are controlled by the contrast in mechanical properties and thickness of the sedimentary beds, rather than by faulting. Bai *et al*. (2000), Underwood *et al* (2003), Huang *et al* (1989), Ladeira *et al* (1981) all reported that mechanical unit thickness or the spacing of mechanical interfaces controls fracture intensity. According to Underwood *et al* (2003), the fracture spacing in layered sedimentary rocks is roughly proportional to the fractured layer thickness with the ratio of spacing to layer thickness ranging from less than 0.1 or greater than 10. In this system the fractures typically occur in parallel sets that span the mechanical thickness, perpendicular to the layer interfaces and are confined to certain lithologies, the fractured units (Helgeson *et al*. 1991, Narr *et al*. 1991, Underwood *et al*. 2003, Wennberg *et al* 2012).

Information about fracture characteristics and distribution are normally obtained from geophysical techniques, which infer fracture attributes from their effects on wave propagation, core description and observation of outcrop analogs (Olson *et al* 2009). These methods are limited in their ability to provide complete information about 3D subsurface fractures and generally depend on statistical correlations to extrapolate results to infer information about subsurface structural conditions (Olson *et al* 2009). This limitation can be addressed, at least in part, by numerical simulation of the fracture formation process using linear elastic fracture modeling. With this tool, the effect of varying combination of mechanical layer thickness and contrast in mechanical properties on fracture characteristics such as spacing and intensity can be studied. This work uses the variational fracture model to simulate fracture formation in a 2D layered model subjected to displacement boundary conditions, mechanical properties and thickness variation of the layers. The mechanical properties of interest are; Poisson's ratio, Young's modulus and fracture toughness.

2. FRACTURE CHARACTERISTICS FROM NUMERICAL SIMULATION

One of the earliest theoretical attempts to explain the formation of opening mode fractures (joints) in layers of different materials is by Hobbs (1967). Hobbs (1967) and Ladeira *et al* (1981) predict a linear relationship between the fracture spacing and bed thickness of sedimentary rocks from an analysis of stress distribution during sequential infilling of fractures in a fracturing material.

Most models for studying fracture characteristics and spacing are built on the foundation of Hobbs' model which is based on an expectation of stress reduction in the region around a pre-existing fracture (i.e. a stress shadow). This hypothesis reasons that since fractures are stress free surfaces, stress in a fractured layer increases from zero on the fracture surface to the far field stress value within a characteristics distance from the fracture face. A new fracture forms only if the stress at a location is greater than the critical magnitude. The stress shadow is a function of the Young's modulus (Hobbs 1967 and Gross *et al*. 1995) of the fractured layer and it inhibits the formation of new fractures at distances closer to the pre-existing fracture than the critical distance of the stress shadow since within this region the stress must be less than the critical magnitude. Gross *et al.* (1995) conducted a series of 2D finite element simulations to determine the distribution of stresses and displacements in a fractured, interbedded rock body and to investigate the effects of contrasting elastic moduli on stress perturbations near the fractures. They obtained good agreement between the numerical results and Hobbs' model. In addition, they found that the lateral extent of the stress reduction shadow and hence, the fracture spacing, is directly proportional to the Young's modulus and the thickness of the fractured layer. It is important to note that their work did not consider the process of fracture formation. Rather, their prediction of fracture spacing was based entirely on analysis of stress distribution (obtained from finite element analysis) in the fractured layer.

Using the theory of elastic-damage mechanics, Tang *et al.* (2008) showed that when fracture spacing to layer thickness ratio in a 3-layer system changes from greater than to less than one, the normal stress acting perpendicular to two pre-existing fractures changes from tensile to compressive. This stress transition, they postulated, precludes further infilling of fractures. Although they studied the influence of fractured layer thickness on fracture spacing, the effect of mechanical stratigraphy on spacing was not studied. Instead, the layer materials were heterogeneous with mechanical properties conforming to a Weibull distribution function. Thus, it was observed that fractures did not occur in parallel sets and were not perpendicular to the layer interface.

Bai *et al*. (2000) also showed that below a critical spacing to layer thickness ratio of one, further fracture infilling is inhibited. They carried out studies on mechanical stratigraphy effect on fracture spacing to layer thickness ratio. Similar to Gross *et al* (1995), their analysis was based on stress transition without simulating the process of fracture formation. In this work, we study the effect of fractured layer thickness and mechanical properties of the layers on the critical average in a multi-layered 2D domain. Critical average spacing is the average distance between the maximum number of vertical fractures obtained before any fracture completely breaks through the material, or before the onset of layer delamination. The fracture formation process that involves fracture initiation, propagation and termination is simulated using the variational model.

3. VARIATIONAL APPROACH TO FRACTURE

The classical Griffith criterion for quasi-static brittle fracture postulates that a fracture propagates along an *a-priori* known path only when the energy release rate (G) reaches a critical value *i.e.* $G = G_c$,.

$$G = \frac{\partial E}{\partial l} \tag{1}$$

where E is the bulk energy and according to Eqn. 1, the energy dissipated to propagate the fracture, proportional to the length in 2D (area in 3D) of the fracture, is supplied by the release of bulk energy. Griffith's criterion however is unreliable on a number of grounds. First the propagation path must be known before hand. Although it assumes fracture propagation is impossible for $G < G_c$, it does not say anything about the case when $G > G_c$. Finally, it is unable to handle fracture initiation in the absence of strong singularities as evident from:

$$\sigma_c = \frac{K_c}{\sqrt{\pi l}} \to \infty \text{ as } l \to 0\,, \tag{2}$$

where σ_c, K_c and l are the critical stress at which material fractures, stress intensity factor and fracture length respectively.

The variational approach recasts Griffith's criterion in a variational setting, i.e. as the minimization over any fracture set (any set of curves in 2D or surfaces in 3D) and any kinematically admissible displacement field u, of a total energy consisting of the sum of the stored potential energy and a surface energy proportional to the fracture length in 2D or area in 3D. If we consider a perfectly brittle linear elastic material with Hooke's Law and critical energy release rate G_c occupying a region Ω of 2D or 3D space, the total energy (F) of this material for any arbitrary number of fractures (Γ) and any kinematically admissible displacement is

$$F(u,\Gamma) = E(u,\Gamma) + G_c H^{N-1}(\Gamma). \tag{3}$$

where $H^{N-1}(\Gamma)$ denotes the fracture length or its surface energy in 3D.

In the variational fracture setting (Francfort and Marigo 1998; Bourdin, Francfort and Marigo 2008), the unilateral minimization of the total energy (Eqn. 3) replaces Griffith's condition of criticality of energy release rate before a fracture can propagate. In addition, it makes no assumption on the number of fractures, the fracture path or their geometry, so provides a unified setting that handles path determination, nucleation, activation and growth of an arbitrary number of fractures in 2D and 3D.

3.1. Numerical implementation

The discontinuity of fracture displacement fields and the unknown location of the discontinuities present difficulties for numerical implementation. To solve this, a phase field representation of the fractures is used. A small regularization parameter ε is introduced and the location of the fracture is represented by a phase field function (v-field; Fig. 1) which takes a value of 0 close to the fracture and 1 far away from the fracture.

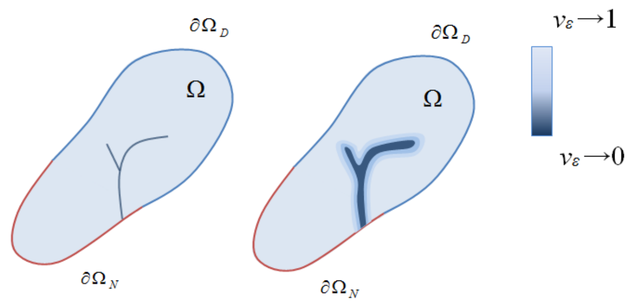

Fig. 1. A) Discrete representation of fractures. B) Phase field (v) representation of fractures.

Considering the v-field in the formulation of the total energy (Eqn. 4), it has been shown (Chambolle, 2004) that Eqn. 4 converges to Eqn. 3 as $\varepsilon \to 0$

$$F_\varepsilon(u,\Gamma) = \int_\Omega v^2 W(u) + G_c \int \frac{(1-v)^2}{2\varepsilon} + \varepsilon |\nabla v|^2\,, \tag{4}$$

where $W(u)$ is the bulk energy density function. Solution of the fracture problem is carried out by an alternating minimization scheme in which the regularized energy (Eqn. 4) is successively minimized with respect to the u (displacement) and v (fracture) fields until convergence is achieved. The regularized problem does not require an explicit representation of the fracture network such as cohesive element or implicit treatment with element enrichment such as extended finite element method. Rather, it is carried out on a fixed mesh and the implementation is based on a structured finite element discretization that is run on parallel computers.

3.2. Variational approach to natural fractures

The computational domain for simulating the fracturing process is shown in Fig. 2. It is a 3-layer rectangular domain with the middle, more brittle layer bounded by two similar less brittle layers. The length of domain is L while the thickness of the middle layer and the two bounding layers are S and T respectively. Thus, the height of the model is 2T+S. In addition to the effect of S and T on the fracture spacing the influence of elastic properties on fracture intensity are studied:

1. Young's modulus of layer A & B, E_f and E_n respectively
2. Poisson's ratio of layer A & B, ν_f and ν_n respectively
3. Fracture toughness of layer A & B, G_{c_f} and G_{c_n} respectively

Loading is implemented by specifying displacements u and $-u$ on the right and left sides of the computational domain while the top and bottom are stress free. Evolution of deformation in the material is quasi-static and is implemented by a monotonically increasing loading through a time function t, which takes values of 1, 2, 3… Thus the displacement loading is given by

$$u(0,t) = -tu$$
$$u(L,t) = tu$$

For all numerical experiments run in this work, the domain is discretized using equal element sizes so that the sample resolution is 0.01 and $u = 0.05m$.

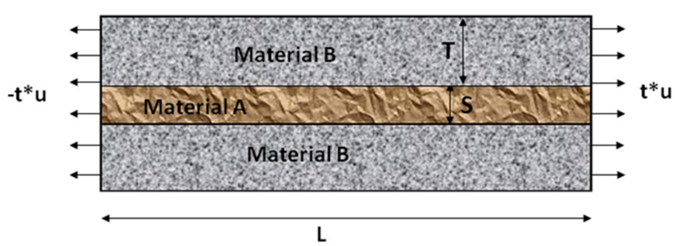

Fig. 2 Geometry and boundary conditions of the computational model.

Table 1. Mechanical properties and domain dimensions for all experiments

Figure	Layer	Gc	E (GPa)	ν	Domain	No. of
5	Middle	0.2	40	0.2	varying	varying
	Bounding	4	40	0.2	varying	varying
6	Middle	0.2	40	equal	5X 0.1	500 X 10
	Bounding	4	40	equal	5 X 0.8	500 X 80
7	Middle	0.2	40	0.25	5 X 0.1	500 X 10
	Bounding	4	40	Varying	5 X 0.8	500 X 80
8	Middle	0.2	40	varying	5 X 0.1	500 X 10
	Bounding	4	40	0.25	5 X 0.8	500 X 80
9	Middle	0.2	varying	0.2	5 X 0.1	500 X 10
	Bounding	4	10	0.2	5 X 0.8	500 X 80
10	Middle	0.2	20,40,60	0.2	5 X 0.1	500 X 10
	Bounding	4	20	0.2	5 X 0.8	500 X 80
12 & 13	Middle	0.2	20,40,60	0.2	varying	varying
	Bounding	4	20	0.2	varying	varying

RESULTS

The series of fracture images in Fig. 3 highlight the important features that are associated with fracture formation in a multi-layered system.

1. Sequential infilling of fractures: Fractures fill up the brittle layer in a sequential manner as documented in Hobbs (1967), Gross (1995) and Tang (2008). As can be observed from Fig. 3, average fracture spacing decreases with increasing strain as new fractures nucleate to infill spaces between pre-existing fractures.
2. Stress build-up between fractures: Built up stress is released by nucleation of fractures as the strain energy is transferred to fracture surface energy. Once a new set of fractures is formed, stress then starts to build up between existing fractures, which leads to formation of another set of fractures, as loading continues. This is highlighted in several images of Figs. 3c and 3e.
3. Parallel fractures, perpendicular to layers: As noted in Underwood (2003), Ruf (1998), Wennberg (2012), Bai (2002), Tang (2008) and Gross (1995) for homogeneous distribution of material properties the simulated fractures form in parallel sets that are perpendicular to the layers.
4. Layer debonding: Layer delamination occurs during the formation of the vertical fractures. In fact, layer delamination affects fracture spacing as additional vertical fracture formation is

inhibited (Tang 2008) since energy is expended in propagating the fractures along the interface, rather than in forming new fractures.

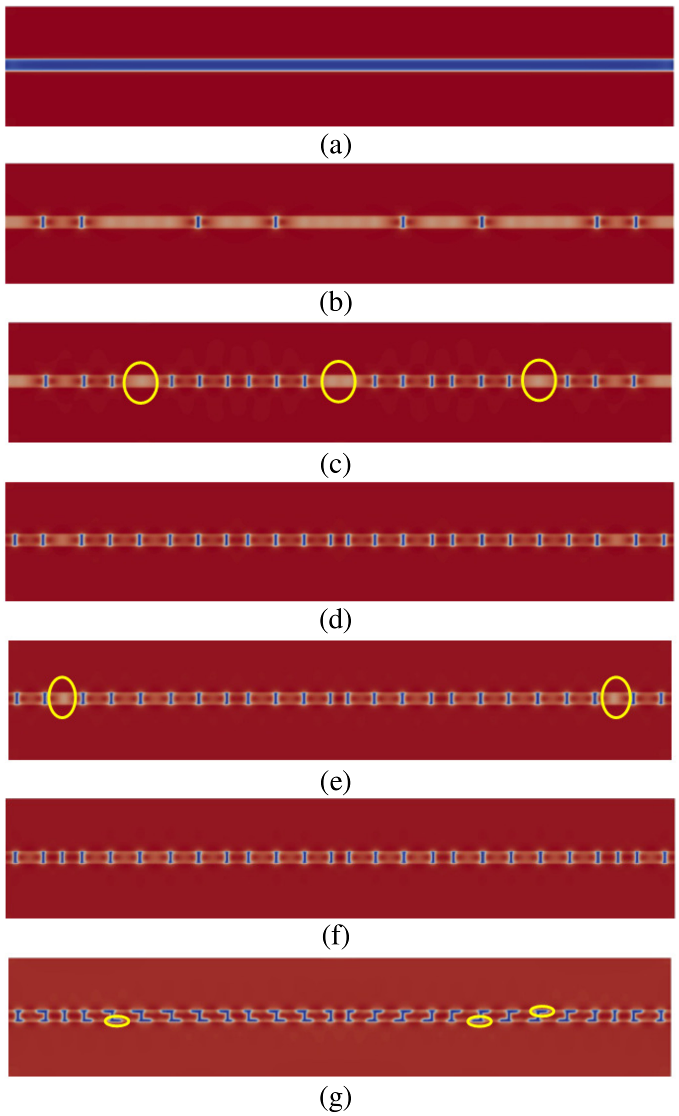

Figure 1. Fracture maps to highlight sequential infilling, stress build-up between adjacent fractures and debonding of layer interface. (a) t=24. (b) t=25. (c) t = 26 (inset shows location where subsequent fractures form during the sequential fracture infilling). (d) t=27. (e) t = 32 (inset highlights stress reduction shadow leading to stress accumulation between pre-existing fractures). (f) t=33. (g) t=49 (inset to highlight layer delamination).

3.3. *Effect of thickness of non-brittle layer*

This numerical experiment was designed to study the impacts of T/S ratio (the ratio of the thickness of the brittle layer to the thickness of the non-brittle layer) on fracture frequency and determine the optimum ratio. Simulations were carried out on the computational domain with a constant value of brittle layer thickness while the thickness of the non-brittle layer was varied for each run. Elastic properties for this case are shown in Table 1 while Fig. 4 shows the fractures generated at different T/S ratios. From Fig. 5, it is seen that the average fracture intensity increases as the thickness of the non-brittle layer increases. However, beyond a T/S ratio of 4, there is little change in fracture intensity with increasing T. Thus, to reduce the number of numerical computations and still obtain results less sensitive to the value of T, we use S = 0.1 and T/S = 4 for subsequent simulations, unless otherwise stated.

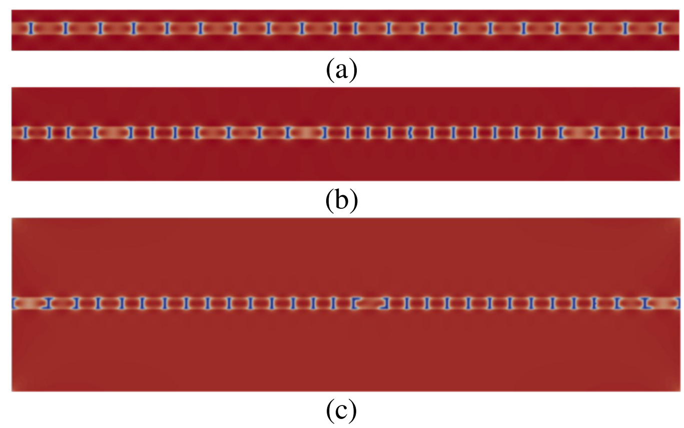

Figure 2. Sequence of fractures obtained at different values of thickness of the bounding layer. (a) T/S = 1. (b) T/S = 3. (c) T/S = 6.

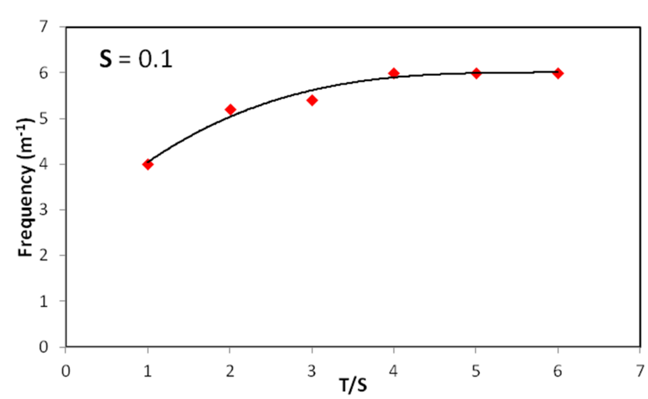

Figure 3. Fracture spacing as a function of the ratio of the thickness of the bounding layer to that of the brittle layer.

3.4. *Effect of poisson's ratio*

Three cases were considered to investigate the influence of the non-fracturing (v_n) and fracturing (v_f) layer Poisson's ratios on fracture spacing. In the first case, the Poisson's ratios of the three layers are equal, and the influence of Poisson's ratio magnitude is investigated. In the second case, the Poisson's ratio of the bounding, non-brittle, layers are kept constant at $\nu_n = 0.25$ while that of the brittle layer is varied for each simulation. In the third case the brittle layer Poisson's ratio is constant at $\nu_f = 0.25$ but the Poisson ratio of the bounding, non-fracturing layers is varied for each simulation. Figs. 6, 7 and 8 show the respective results for the three cases while the elastic properties used for the simulations are also presented in Table 1. From Fig. 6, minimum fracture spacing is obtained at a Poisson's ratio of about 0.07 (i.e. $\nu_n = \nu_f = 0.07$). Beyond this value, a linear trend is observed with increasing fracture spacing at increasing values of the Poisson's ratio while below this value, fracture spacing increases with decreasing Poisson's ratio. Fig. 7 shows that at a ν_f/ν_n ratio greater than 3.5 the fracture spacing remains fairly constant. Below this value, fracture spacing decreases rapidly with decreasing ratio values. Finally, a fairly linear trend is observed in the data of Fig. 8 at a ratio of Poisson's ratio of the bounding layer to that of the brittle layer greater than 2.5. Within this range, the fracture spacing increases as the ratio value increases. A lot of scatter is observed in data below the ratio value of 0.25.

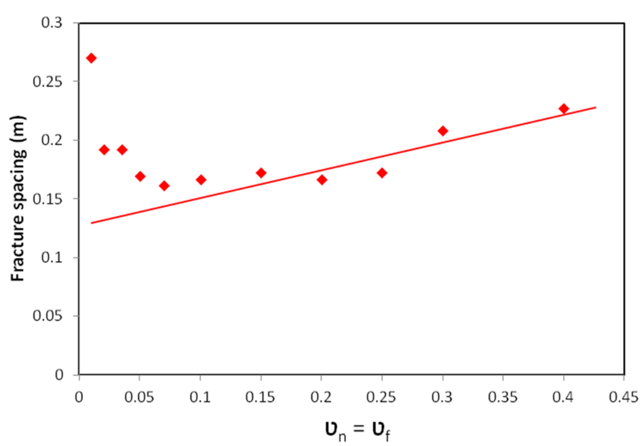

Figure 4. Fracture spacing as a function of Poisson's ratio. Poisson's ratios of the 3 layers are equal.

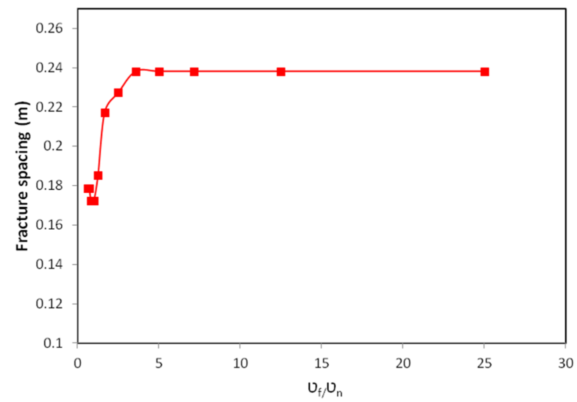

Figure 5. Fracture spacing as a function of Poisson's ratio. Poisson's ratio of the middle layer is constant at 0.25.

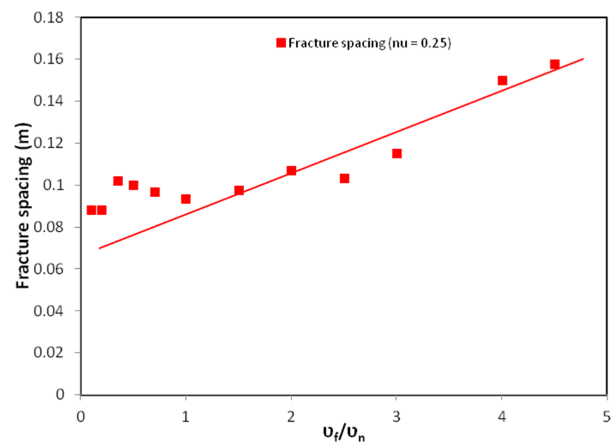

Figure 6. Fracture spacing as a function of Poisson's ratio. Poisson's ratio of the bounding layer is constant at 0.25.

3.5. *Effect of Young's moduli*

The effects of the Young's moduli of the brittle layer and the neighboring non brittle layers is studied by varying the value of the Young's modulus in the brittle layer while keeping that of the bounding layers constant at a value of 10GPa. From Fig. 9, the critical average fracture spacing increases monotonically with increase in Young's modulus. This finding is related to the stress reduction shadow postulated by Hobbs' model for which Gross *et al* (1995) and Tang *et al*. (2008) showed that its lateral extent (fracture spacing) is directly proportional to the ratio of the Young's modulus of the brittle layer to that of the non-brittle layer.

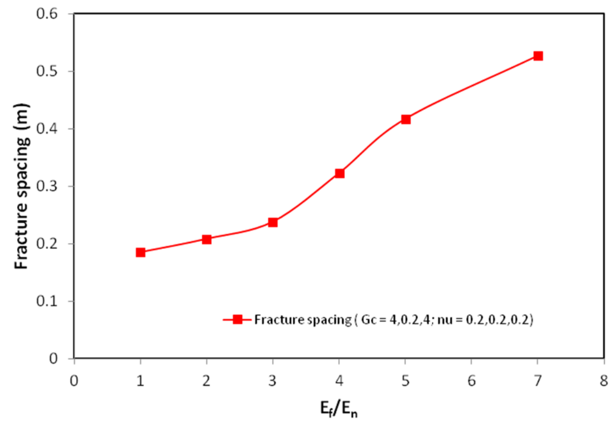

Figure 7. Fracture spacing as a function of the ratio of Young's moduli of the middle and bounding layers respectively.

3.6. *Effect of Fracture Toughness*

Fracture toughness determines the brittleness of a rock. Brittle rocks are less resistant to failure and thus have smaller fracture toughness compared to less or non-brittle rocks. This explains why the middle layer in our computational model is more brittle compared to the adjourning, bounding layers. To investigate the contribution of fracture toughness, the toughness of the bounding layer is kept constant at $G_{c_f} = 4GPa.m$ while the value of the brittle, middle layer is varied. From the results in Fig. 10**,** it is observed that in addition to the general trend of reducing fracture spacing with increasing ratio of the toughness of the bounding layer to that of the middle layer, the influence of the fracture toughness on spacing diminishes as this ratio increases.

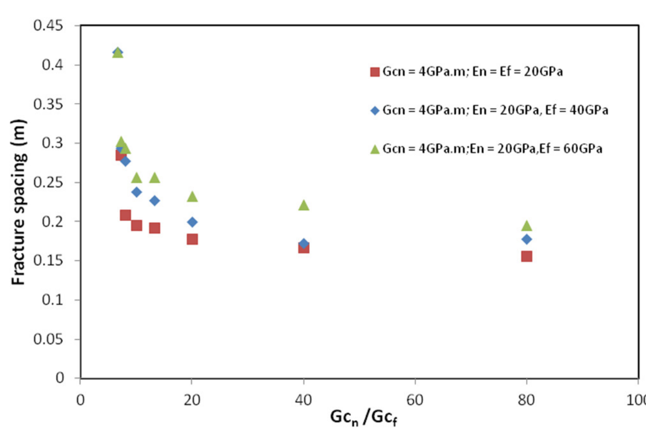

Figure 8 Fracture spacing as a function of the ratio of fracture toughness of the middle and bounding layers respectively for 3 cases with different middle layer Young's modulus.

3.7. *Bed thickness*

As mentioned earlier, several authors (Ladeira *et al.* 1981; Hobbs 1967; Bai *et al.* 2000, 2002; Ruf *et al.* 1998) have suggested that spacing in brittle rocks is affected by the thickness of the fractured layer. Different relationships between the two have been proposed, ranging from linear to negative exponential forms. The linear relationship is most widely accepted, as field data have been shown to follow this behavior and most data in literature scatter around the linear trend (see for example Ruf *et al*., 1998).

To better understand the effect of the thickness of the brittle layer on bed thickness, we ran a number of simulations while varying S from Fig. 1. Results for this experiment are shown in Fig. 11. The results agree with those of earlier works in that there is monotonic increase in fracture spacing with bed thickness. We also observe that this relationship is dependent on the mechanical properties of the layers as the spacing increases with increase in the ratio of Young's modulus of the brittle layer to that of the bounding, non-brittle layer. In addition, for the cases of equal Young's moduli in all three layers, the spacing increases with a decrease in the Young's modulus value. Furthermore, the fracture spacing decreases if the ratio of the fracture toughness of the bounding layers to that of the brittle layer increases. Whilst a similar trend for different elastic property contrast is obtained for all cases run, the predicted relationship between the fracture spacing and bed thickness is far from linear. In fact, as shown in Fig. 12, the modeling results are best fitted by a quadratic function. We reiterate that data for these plots are obtained by simulating the process of fracture formation using the variational fracture model, which autonomously nucleates and propagates fractures as minima of the global energy system.

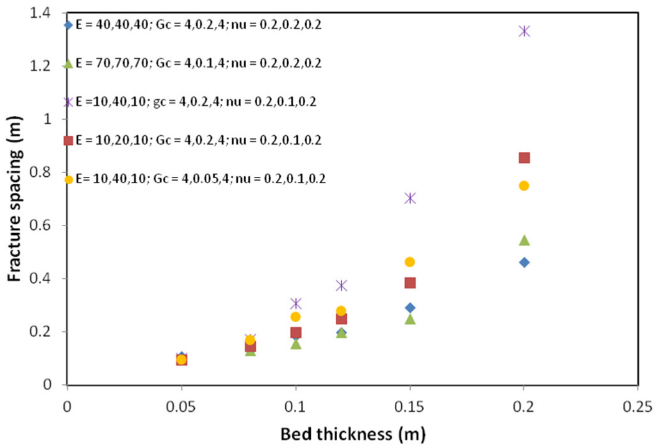

Figure 91. Fracture spacing as a function of bed thickness for 5 different cases of Young's moduli.

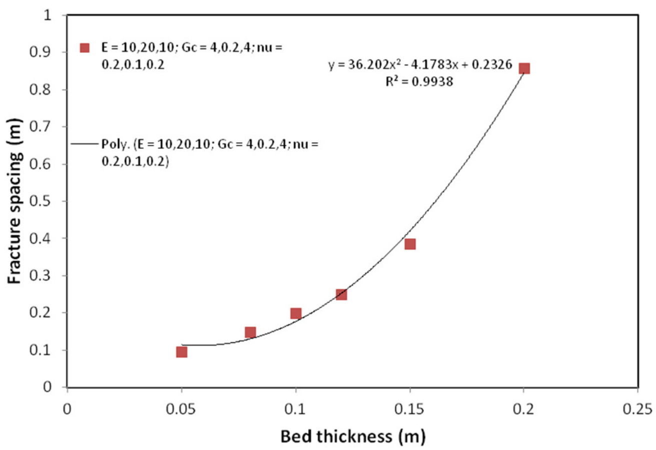

Figure 102. Fracture spacing as a function of bed thickness and a polynomial model fit to the function.

3.8. *Pre-existing fractures*

In this case, we predict the propagation path of pre-existing fractures in the brittle layer. The distribution of initial fractures is shown in Fig. 13a while the fracture state after applied strain of 8.33E-5 and 1.45E-3 respectively are shown in Figs. 13b and 13c. As seen in Fig. 13a, propagation proceeds to the top boundary layer interface from the fracture on the left side of the image. Upon short propagation along the top interface, the middle fracture starts to feel the influence of the left fracture and is attracted to it. It coalesces with the left fracture at an angle perpendicular to the plane of the middle fracture. After the two fractures are joined, they propagate through the bottom interface to the side of the smallest fracture on the right side of the image. Propagation of the fracture beside the smallest fracture creates a stress reduction shadow around it, which inhibits its propagation.

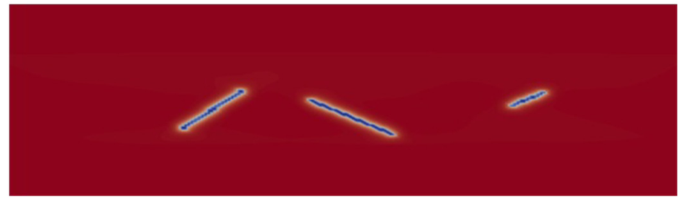

(a)

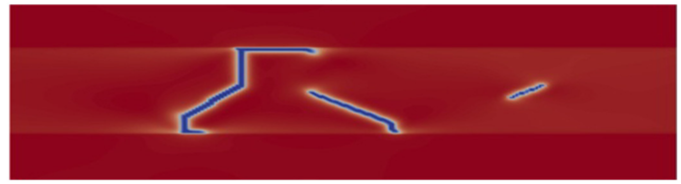

(b)

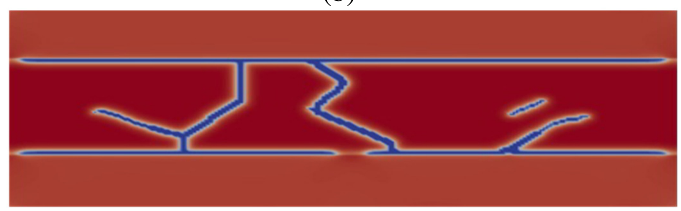

(c)

Figure 13. Fracture propagation given pre-existing fractures. (a) initial distribution of pre-existing fractures. (b) fracture map after applied strain of 8.33E-5. (c) fracture map after applied strain of 1.45E-3.

3.9. *Multi-layer*

As shown in Fig. 14, the distribution of fracture spacing in the layers is a function of the bed thickness, the mechanical properties of the layers, and the strain, leading to varied fracture spacing in the different layers. In this final experiment, we simulate fractures in a 9–layer system with different mechanical properties. The layers are arranged by alternate distribution or brittle and non-brittle layers. The brittle layers are arranged in a way that the brittleness (*i.e.* lower fracture toughness and higher Young's modulus) reduces from top to bottom. From Fig. 15a, the fracture spacing increases from the top brittle layer to the bottom brittle layer and this trend agrees with prior discussion of mechanical influence on fracture spacing. After applying further strain, a through-going fracture is formed, connecting fractures on the right hand side of the image, which cuts completely through the material (Fig. 15b). After the through-going fracture cuts the layers, the material experienced no additional fracture formation.

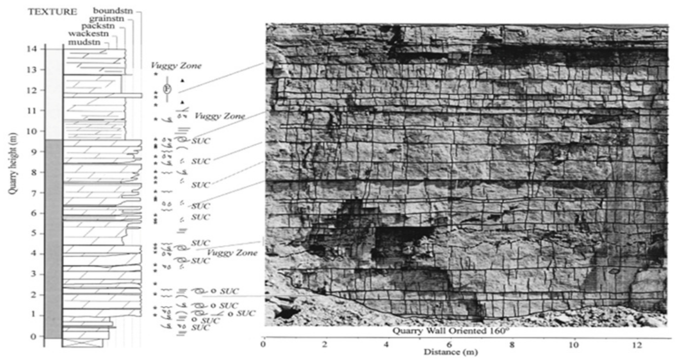

Figure 14. Stratigraphic section and fracture distribution (Underwood *et al.* AAPG Bulletin 87, No. 1 (2003) 121-142. AAPG©2003, reprinted by permission of the AAPG whose permission is required for further use)

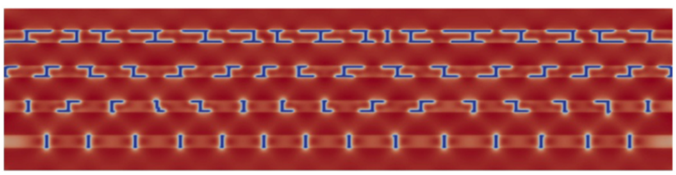

(a)

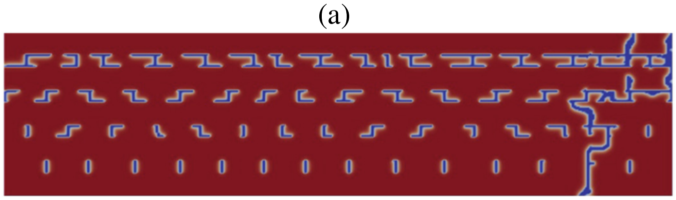

(b)

Figure 15. Fracture distribution in multi-layer system. (a) fracture image after applied strain of 1.5E-3 (b) fracture image after applied strain of 2.45E-3.

4. SUMMARY AND CONCLUSIONS

We have demonstrated the ability of the variational fracture model to simulate initiation, propagation and termination of fractures in a brittle material. In addition, the numerical simulations predict sequential infilling of fractures, stress build-up between adjacent fractures, fracture occurrence in parallel sets that are perpendicular to layers interfaces. These features are all associated with fracture formation in multi-layered systems subjected to mechanical loading on the boundaries. In addition, debonding of the interfaces is shown to occur during fracture formation, a process that drives the brittle layers to fracture saturation faster as more energy is expended in propagating the fractures along the boundary. This energy otherwise would have been expended in creating new vertical fractures. Using information about the number of fractures generated from the numerical simulations, the critical average spacing at fracture saturation is calculated as a function of the mechanical properties of the layered material and the thickness of the layers. From the numerical simulations it appears that the model of a linear relationship between fracture spacing and bed thickness as derived from field observation might be incorrect as we obtained a quadratic relationship between average fracture spacing and bed thickness. Our numerical results support the stress reduction shadow dependence on Young's modulus of the brittle layer as we obtained a monotonic reduction in fracture spacing with decrease in the ratio of the Young's modulus of the brittle layer to that of the bounding, non- brittle layers. In contrast, the dependence of fracture spacing on Poisson's ratio is not clear-cut. However, within certain ranges of the data, a linear relationship between the two parameters is obtainable.

REFERENCES

1. Bai, T., Maerten, L., Gross, M., and Aydin, A. "Orthogonal cross joints: do they imply a regional stress rotation?". J. of Struct. Geol. 24 (2002) 77-88.

2. Bai,T., Pollard, D. D. "Fracture spacing in layered rocks: a new explanation based on the stress transition". J. of Struct. Geol. 22 (2000) 43-57.

3. Becker, A., and Gross, M. R. "Mechanisms for joint saturation in mechanically layered rocks: an example from southern Israel". 257 (1996) 223-237.

4. Bourdin B., Francfort G. A., and Marigo J. –J. "The variational approach to fracture". (reprinted from J. Elasticity) Springer 91 (1-3) (2008) 1-148.

5. Chambolle, A. "An approximation result for special functions," J. Math Pures. Appl. 83, 929-954 (2004).

6. Francfort, G.A., and Marigo, J. –J. "Revisiting brittle fracture as an energy minimization problem" J. Mech. Phys. 46 (1998) 1319-1342.

7. Gross, M. R., Fischer, M. P., and Engelder, T. "Factors controlling joint spacing in interbedded sedimentary rocks: integrating numerical models with field observations from the Monterey formation, USA". Geol Soc. Special Publ. No. 92 (1995) 215-233.

8. Huang Q., and Angelier, J. "Fracture spacing and its relation to bed thickness". Geological Magazine. 126 (1989) 355-362.

9. Helgeson, D. E., and Aydin, A. "Characteristics of joint propagation across layer interfaces in sedimentary rocks". J. of Struct. Geol. 13, No. 8 (1991) 897-911.

10. Hobbs, D. W. "The formation of tension joint in sedimentary rocks: an explanation". Geological Magazine. 104, (1967) 550-556.

11. Ladeira, F. L., and Price, N. J. “Relationship between fracture spacing and bed thickness”. J. of Struct. Geol. 3 (1981) 179-183.

12. Narr, W., and Supe, J. “Joint spacing in sedimentary rocks”. J. of Struct. Geol. 11, No. 9, (1991) 1037-1048.

13. Nelson, R. A. “Geologic analysis of naturally fractured reservoirs”. Gulf Professional Publishing 2nd Ed. (2001).

14. Olson, J. E., Laubach, S. E., and Robert, H. “Natural fracture characterization in tight gas sandstones: integrating mechanics and diagenesis”. Lander. AAPG 93, No. 11 (2009) 1535-1549.

15. Priest, S. D., Hudson, J. A. “Discontinuity spacings in rock”. Int. J. Rock Mech. Min Sci. & Geomech. 13 (1976) 135-148.

16. Ruf, J. C, Rust, K. A., and Engelder, T. “Investigating the effect of mechanical discontinuities on joint spacing”. Tectonophysics 295 (1998) 245-257.

17. Tang, C. A., Liang, Z. Z., Zhang, Y. B., Chang, X., Tao, X., Wang, D. G., Zhang, J. X., Liu, J. S., Zhu, W. C., and Elsworth, D. “Fracture spacing in layered materials: A new explanation based on two-dimensional failure modeling”. Ame. J. of Sci. 308 (2008) P. 49-72.

18. Underwood, C. A., Cooke M. L., Simo, J. A. and Muldoon, M. A. “Stratigraphic controls on vertical fracture patterns in Silurian dolomite, northeastern Wisconsin”. AAPG Bulletin 87, No. 1 (2003) 121-142.

19. Wennberg, O.P., Svana, T., Azizzadeh, M., Aqrawi, A. M. M., Brockbank, P., Lyslo, K. B., and Ogilvie, S. “Fracture intensity vs. mechanical stratigraphy I nplatform top carbonates: the Aquitanian of the Asmari Formation, Khaviz Anticline, Zagros, SW Iran”. Petroleum Geoscience (2012) 235-246.